Supplementary Information

Successful anti-PD-1 Cancer Immunotherapy Requires T Cell-Dendritic Cell Crosstalk Involving the Cytokines IFN-γ and IL-12

Christopher S. Garris*, Sean P. Arlauckas*, Rainer Kohler, Marcel P. Trefny, Seth Garren, Cécile Piot, Camilla Engblom, Christina Pfirschke, Marie Siwicki, Jeremy Gungabeesoon, Gordon J. Freeman, Sarah E. Warren, SuFey Ong, Erica Browning, Christopher G. Twitty, Robert H. Pierce, Mai H. Le, Alain P. Algazi, Adil I. Daud, Sara I. Pai, Alfred Zippelius, Ralph Weissleder, Mikael J. Pittet#

*These authors contributed equally
#Corresponding author

Supplemental Figures

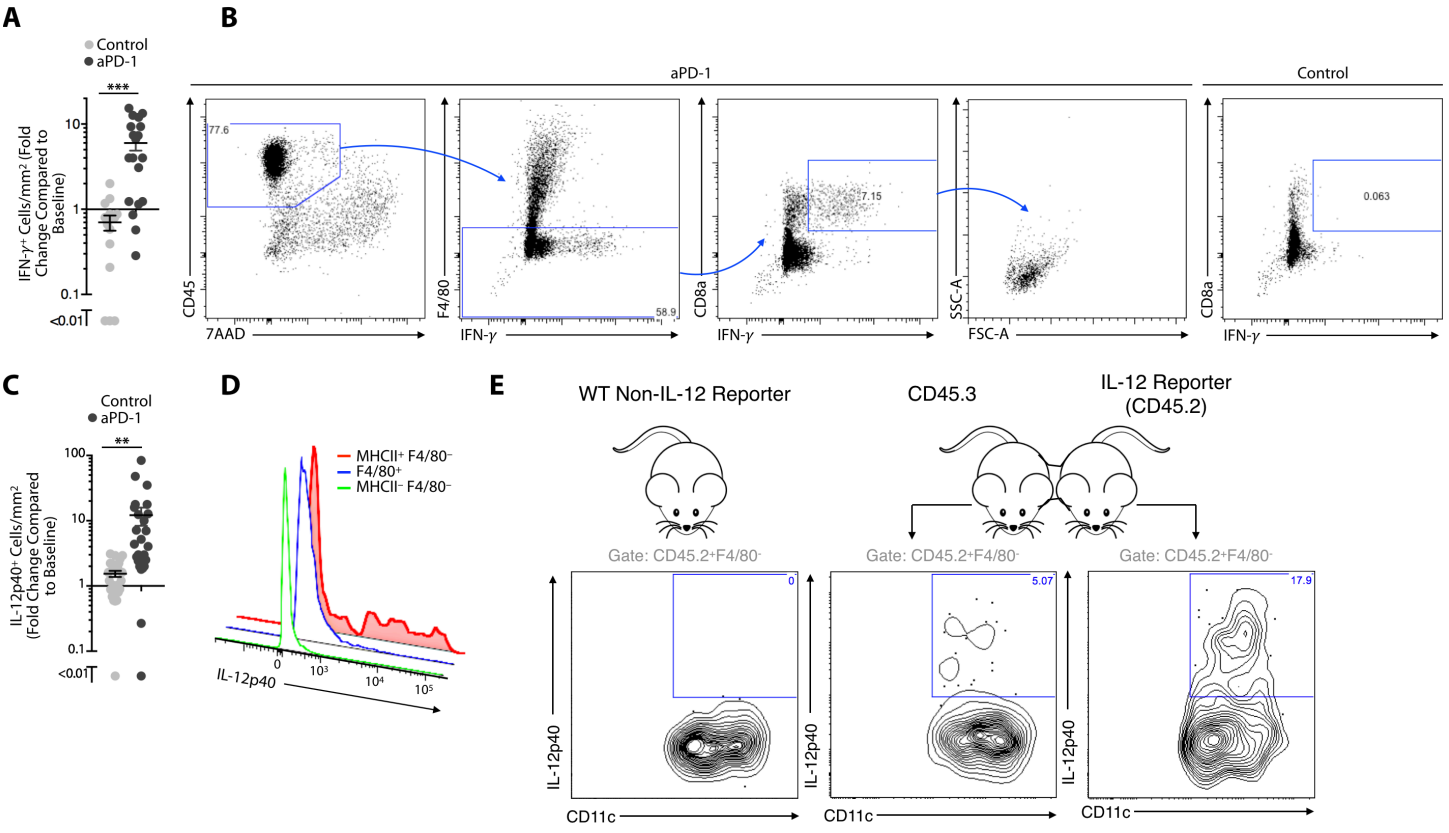

Fig. S1. Related to Figure 1. Characterization of IFN-γ^+ CD8$^+$ T Cells and IL-12p40$^+$ DCs After aPD-1 Therapy. (A) Quantification of IFN-γ signal from intravital microscopy of IFN-γ reporter mice treated or not with aPD-1 mAbs (n = 3 mice/group). Cell counts are expressed as fold change of IFN-γ^+ cells/mm^2 from pre-treatment baseline. **(B)** Flow cytometry of aPD-1-treated MC38 tumors from IFN-γ reporter mice shows IFN-γ expression by CD8α$^+$ cells. Gating strategy for IFN-γ^+ cells is shown for an aPD-1 treated sample. **(C)** IL-12p40$^+$ cells per mm^2 were quantified using intravital microscopy of MC38 tumors in IL-12p40 reporter mice treated with and without aPD-1 treatment. Values were calculated as a fold change from pre-treatment baseline (n = 5 mice/group). IL-12 and IL-23 share the p40 subunit but have contrasting roles in cancer immunity, with IL-12 as antitumor and IL-23 as pro-tumor (Yan et al., 2017). Our data indicate responses due to IL-12 biological activity considering the lack of detectable IL-23 production in this experimental setting (Figure S2A) and association of IL-12p40 with an anti-tumor response. **(D)** IL-12p40 reporter mice bearing MC38 tumors were treated with aPD-1 and tumors were harvested 3 days after treatment. Single cell suspensions of the tumors were prepared and stained for flow cytometry. Shown are the following subsets cells (pre-gated on CD45$^+$): MHCII$^+$ F4/80$^-$ (red), F4/80$^+$ (blue) and MHCII$^-$ F4/80$^-$ (green). **(E)** Congenic CD45.3 and IL-12p40 reporter mice were parabiosed and implanted with MC38 tumors. Mice were then treated with aPD-1 and tumors were isolated for flow cytometry analysis of IL-12-producing cells. Data are representative of 3 parabiotic mouse pairings. ** p-value < 0.01, *Student's* t-test two tailed.

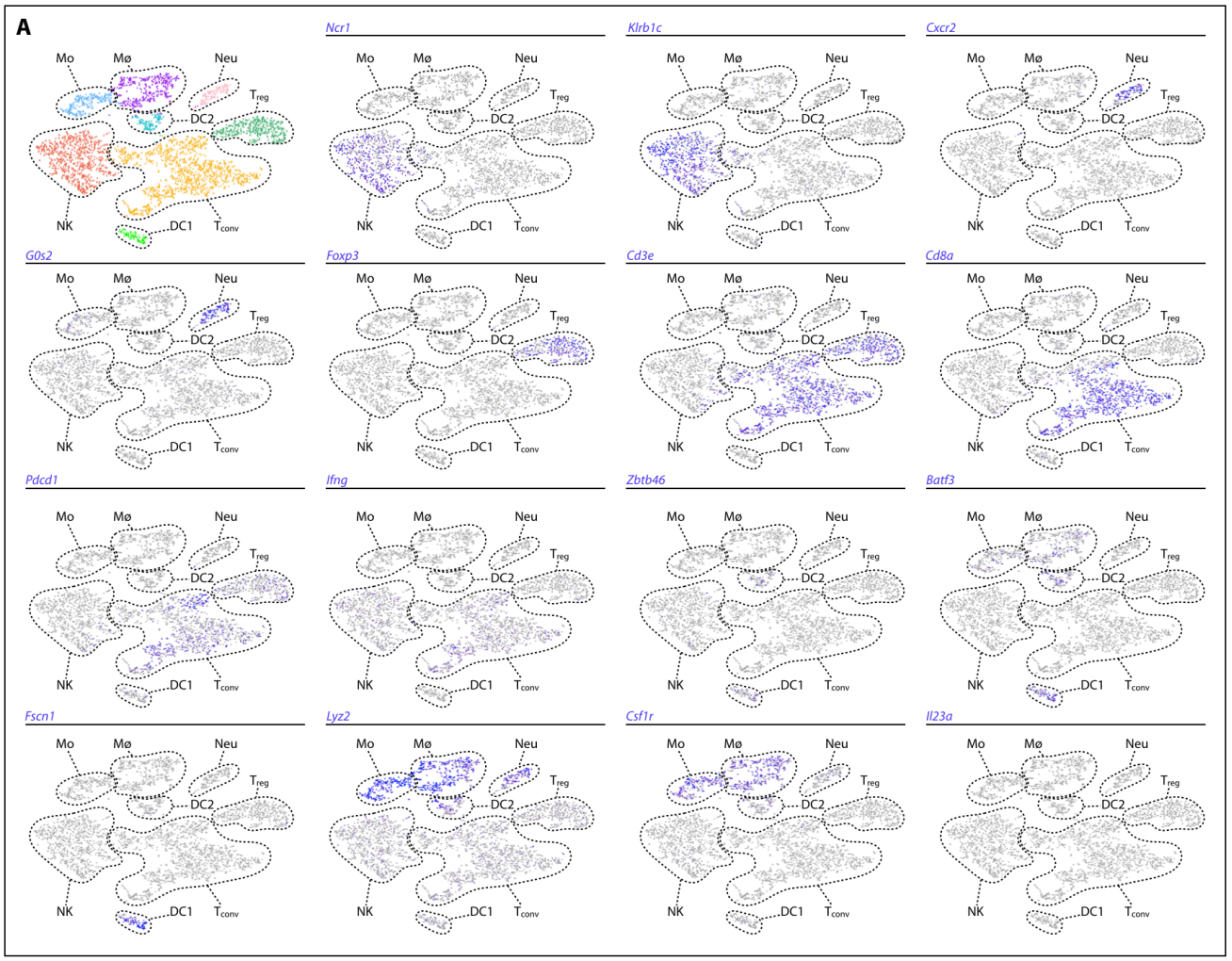
A
Mo
Mø
Neu
Treg
DC2
NK
DC1
Tconv
Ncr1
Klrb1c
Cxcr2
G0s2
Foxp3
Cd3e
Cd8a
Pdcd1
Ifng
Zbtb46
Batf3
Fscn1
Lyz2
Csf1r
Il23a

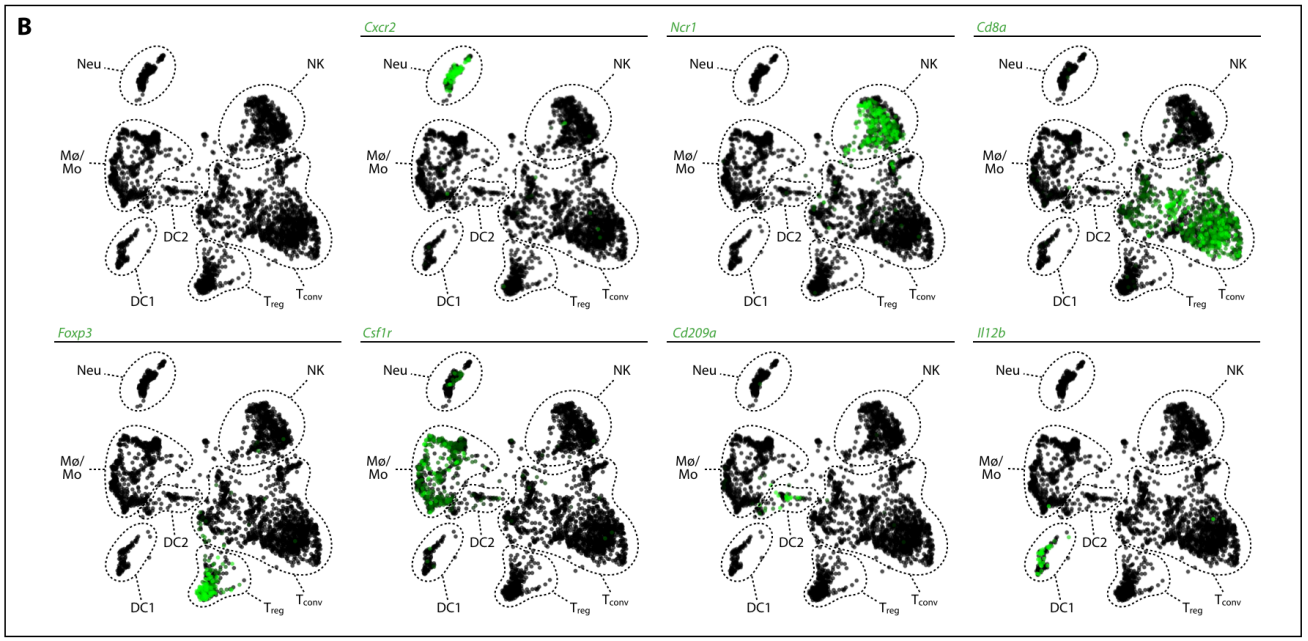
B
Neu
NK
Mø/
Mo
DC2
DC1
Treg
Tconv
Cxcr2
Ncr1
Cd8a
Foxp3
Csf1r
Cd209a
Il12b

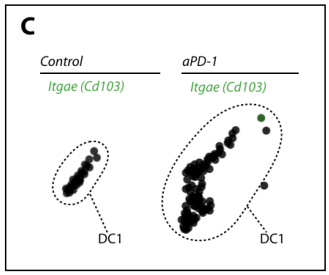
C
Control
aPD-1
Itgae (Cd103)
DC1

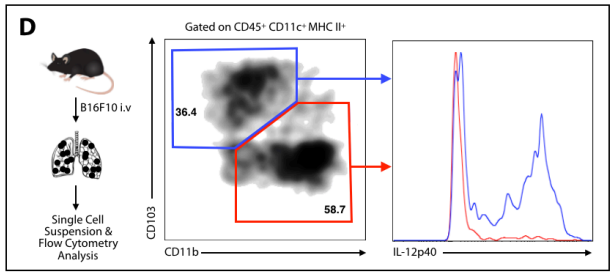
D
Gated on CD45+ CD11c+ MHC II+
B16F10 i.v
Single Cell
Suspension &
Flow Cytometry
Analysis
36.4
58.7
CD103
CD11b
IL-12p40

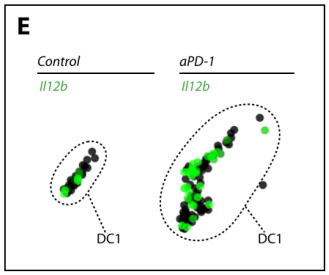
E
Control
aPD-1
Il12b
DC1

Fig. S2. Related to Figure 2. Characterization of scRNA Sequencing of MC38 Tumor Immune Infiltrates. **(A)** t-stochastic neighbor embedding (t-SNE) feature plots are clustered according to cell lineage defining factors, and assigned to immune cell types. Examples of defining factors are enumerated, and correspond to NK populations, *Ncr1* and *Klrb1c*; Neutrophil populations, *Cxcr2* and *G0s2*; T regulatory cells, *Foxp3*; T conventional cells, *Cd3e*, *Cd8a*, *Pdcd1* and *Ifng*; Dendritic Cells, *Zbtb46*, *Batf3* and *Fscn1*, and Monocytes/ Macrophages, *Lyz2* and *Csf1r*. *Il23a* is shown as control. DC, dendritic cell; Mø, macrophage; Mo, monocyte; Neu, neutrophil; NK, natural killer cell; Tconv, conventional T cell; Treg, regulatory T cell. **(B)** SPRING plots of selected cluster defining transcripts. Neutrophils, *Cxcr2;* NK cells, *Ncr1;* $CD8^+$ T cells, *Cd8a;* T regulatory cells, *Foxp3*; Macrophages and monocytes, *Csf1r*; DC1, *Il12b*; DC2, *Cd209a.* Green colored dots identify cells expressing each respective factor. DC, dendritic cell; Mø, macrophage; Mo, monocyte; Neu, neutrophil; NK, natural killer cell; Tconv, conventional T cell; Treg, regulatory T cell. **(C)** *Itgae (Cd103)* expression in DC1 cells identified by SPRING analysis either in control (left) or aPD-1 treated (right) animals. **(D)** IL-12p40 reporter mice were injected i.v. with B16F10 cells and lungs were processed for flow cytometry after 10 days of tumor growth. DCs were separated into $CD103^+$ $CD11b^-$ (blue) and $CD103^-$ $CD11b^+$ (red) subsets. Histograms show IL-12p40 expression in these subsets. Plots are representative of 5 mice. **(E)** Same as in (C) but for *Il12b* expression.

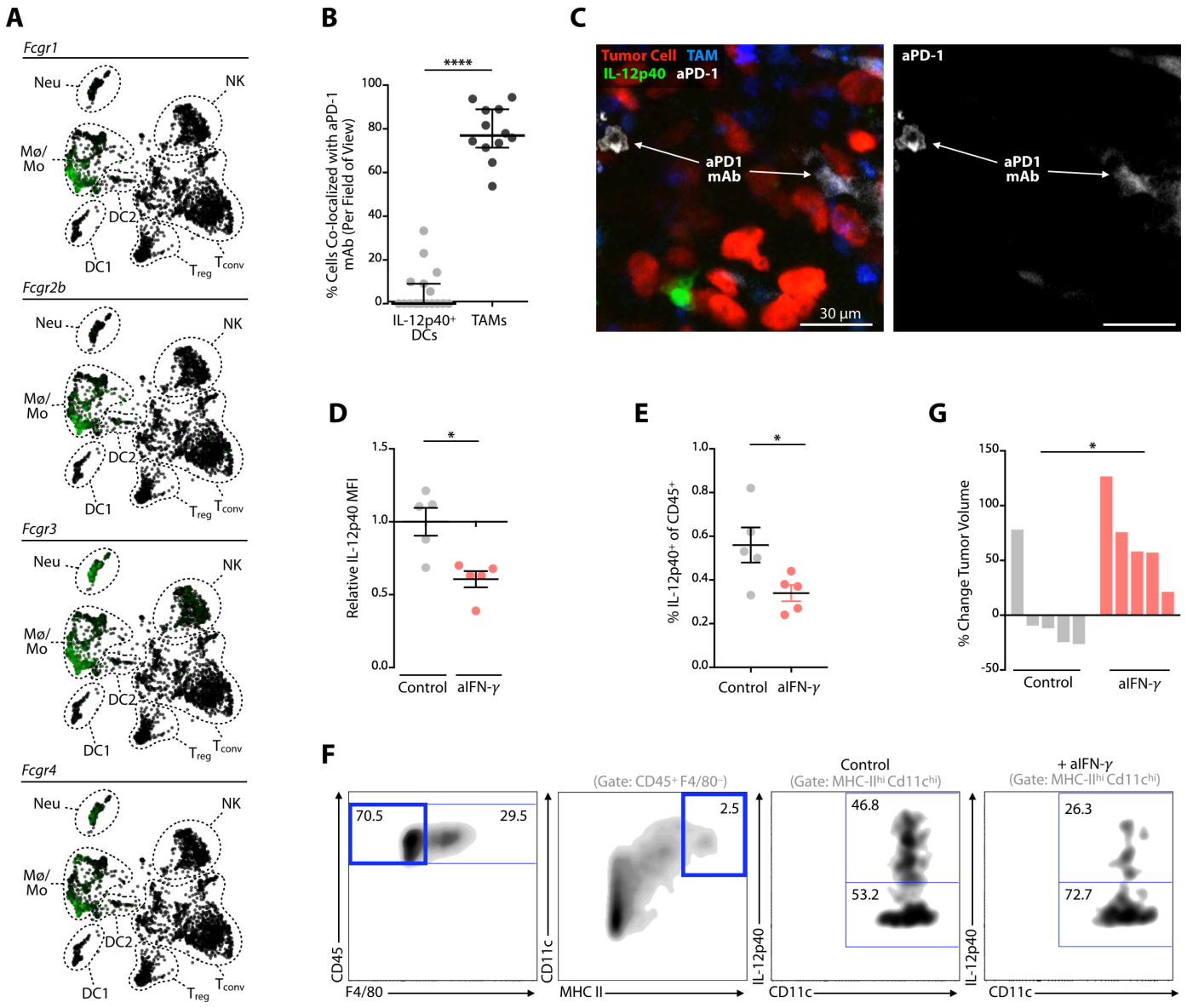

Fig. S3. Related to Figure 3. aPD-1 Induces IL-12 Production Indirectly through IFN-γ Signaling. (A) The expression pattern of selected murine Fc receptors across immune cells clustered using SPRING analysis of MC38 tumor immune infiltrates analyzed by scRNA seq. **(B)** H2B-mApple MC38 tumor-bearing IL-12p40 reporter mice were treated with AlexaFluor647-aPD-1 mAbs and analyzed by intravital imaging. The data show the percent of aPD-1 signal overlapping with IL-12p40$^+$ cells or with tumor-associated macrophages (TAMs) 24 h after aPD-1 administration. **(C)** AF647-aPD-1 mAb was administered to IL-12p40 reporter mice bearing H2B-mApple MC38 tumors and *in vivo* microscopy images above represent drug distribution within the first hour of administration. Red, MC38 tumor cells; blue, tumor associated macrophages (TAM); green, IL-12p40$^+$ cells; white, AF647-aPD-1 mAb. Scale bars represent 30 μm. **(D)** Flow cytometry measurement of IL-12p40 signal (MFI, mean fluorescent intensity) in MC38 tumors three days after aPD-1 treatment and in the presence or absence of IFN-γ neutralizing mAbs (aIFN-γ). Data normalized to baseline IL-12p40 levels from n = 5 mice per group. **(E)** Flow cytometry of IL-12$^+$ cells as a proportion of CD45$^+$ cells, using IL-12p40 reporter mice. **(F)** MC38 tumor bearing IL-12p40 reporter mice were treated with aPD-1, with or without co-administration of aIFN-γ. Tumors were collected for flow cytometry and DC populations were defined as CD45$^+$ F4/80$^-$ CD11c^{hi} MHCII^{hi}. Shown are two representative plots of control and aIFN-γ conditions from n = 5 per group, data correspond to Figure 3D. **(G)** Tumor growth of indicated animals at 3 days post aPD-1 treatment with or without aIFN-γ. Tumor size of each individual animal defines pre-treatment baseline and values reported are changes from baseline after treatment; n = 5 mice per group. * p-value < 0.05, **** p < 0.001 *Student's* two-tailed, t-test.

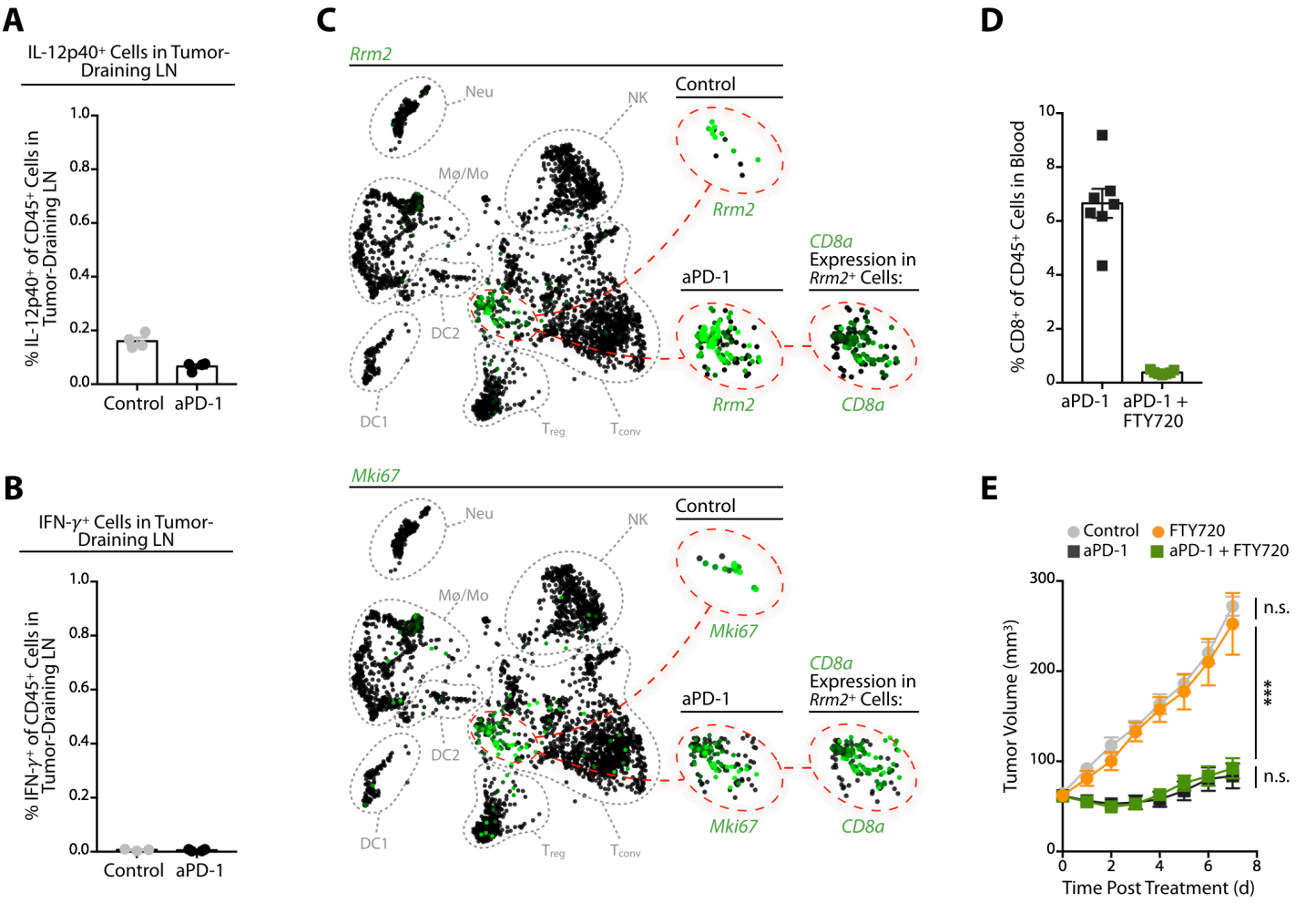

Fig. S4. Related to Figure 4. IL-12 Responses to aPD-1 mAbs Do Not Occur in the Lymph Node and aPD-1 Treatment Functions Independently of Lymphocyte Recirculation. (A) MC38 tumor-bearing IL-12 reporter mice were treated with aPD-1 or not (control), and tumor-draining lymph nodes were harvested 48 hours after treatment. Flow cytometry of IL-12$^+$ DCs is shown with control (grey) and aPD-1 (black) treatments; n = 4 mice/group. **(B)** MC38 tumor-bearing IFN-γ reporter mice were treated with aPD-1 or not (control) and tumor-draining lymph nodes were harvested 48 hours after treatment. Flow cytometry of IFN-γ^+ cells is shown with control (grey) and aPD-1 (black) treatments; n ≥ 3 mice/group. **(C)** Single cell RNA sequencing expression data of the proliferation associated genes *Rrm2* and *Mki67* within tumor immune cell populations. Comparisons are from samples treated or not with aPD-1. Cell clusters positive for either *Rrm2* or *Mki*67 are also shown to express *Cd8a*. **(D)** Blood of aPD-1-treated animals without (black) or with (green) FTY720 was analyzed by flow cytometry for circulating CD8$^+$ T cells; n ≥ 7 mice/group. **(E)** Tumor growth curves of MC38 tumor-bearing mice that received FTY720 alone (orange circle), aPD-1 alone (black square), both aPD-1 and FTY720 (green square), or that were left untreated (control, grey circle); n ≥ 6 mice/group from one experiment. n.s = not significant, *** $p < 0.001$. One way ANOVA with multiple comparisons.

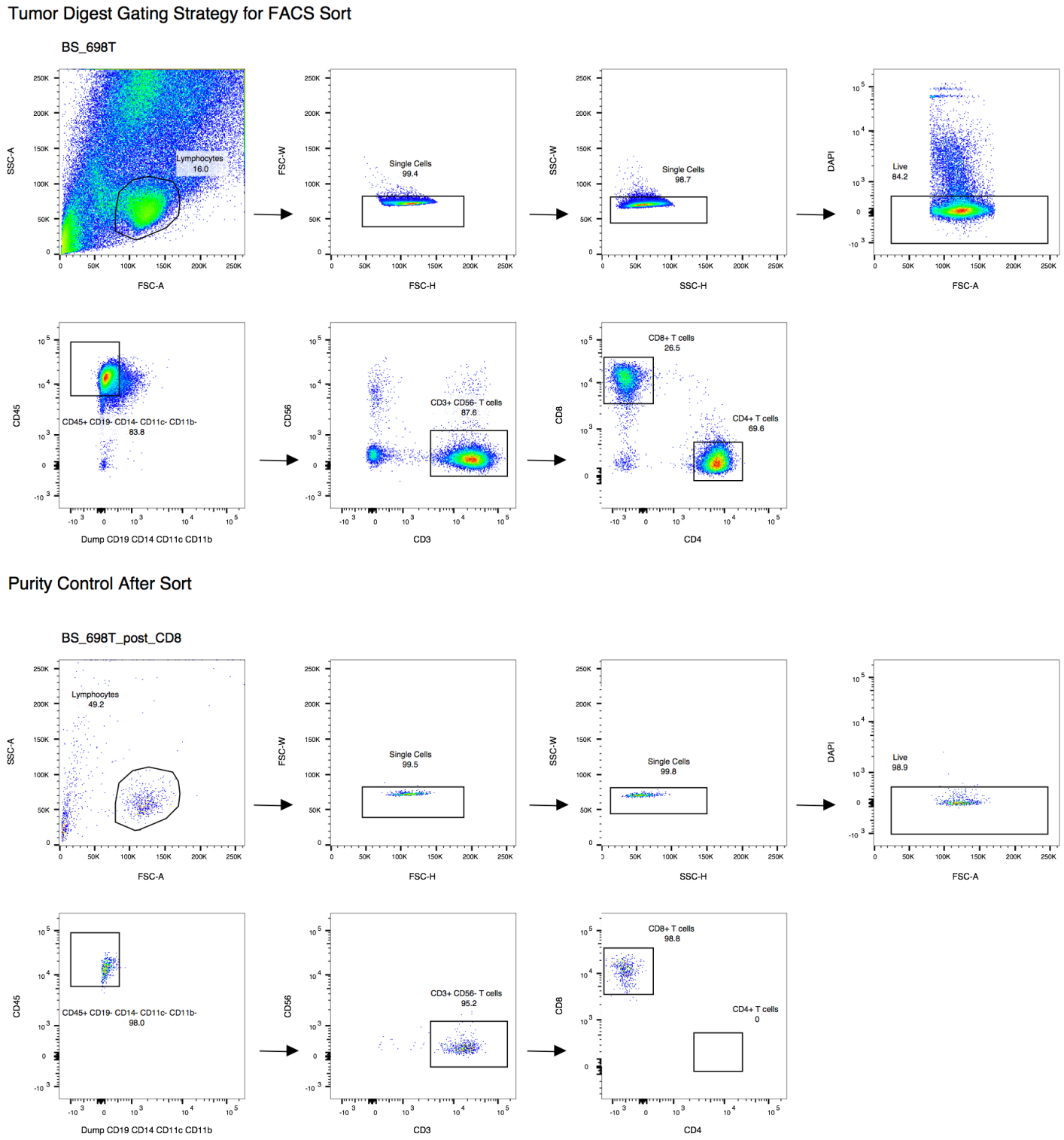

Fig. S5. Related to Figure 5. Flow Cytometry Sorting Strategy and Validation of Human Tumor Infiltrating Lymphocytes. Fresh tumor samples isolated from cancer patients were mechanically dissociated and digested into single cell suspensions, and the representative flow cytometry gating strategies for isolating $CD8^+$ T cells. Samples were re-run through the initial gating strategy to ensure sample purity.

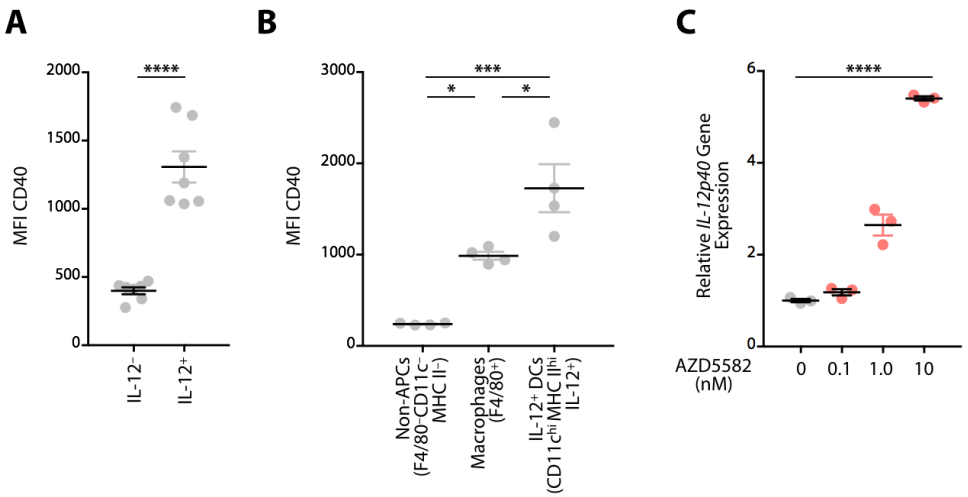

Fig. S6. Related to Figure 6. IL-12 Expressing Cells Express More CD40 and AZD5882 can Induce IL-12 Production In vitro. (A) Flow cytometry of MC38 tumors from IL-12p40-eYFP reporter mice, stained for CD40 expression; n = 7 per group. **(B)** Flow cytometry of CD40 expression from the following tumor immune cell populations: Non-Antigen Presenting Cells (non-APCs, defined as F4/80$^-$ CD11c$^-$ MHCII$^-$), macrophages (F4/80$^+$) and IL-12$^+$ DCs (CD11c^{hi} MHCII^{hi} IL-12$^+$); n = 4 per group. **(C)** Flt3L-derived bone marrow DCs were cultured in vitro with various concentrations of AZD5582 for 24 hours, and were harvested for RNA. Shown is fold change expression of IL-12p40 transcripts compared to untreated conditions (n = 3 per condition). Results are representative of at least 2 independent experiments. **** $p < 0.0001$; *Student's* two tailed t-test.

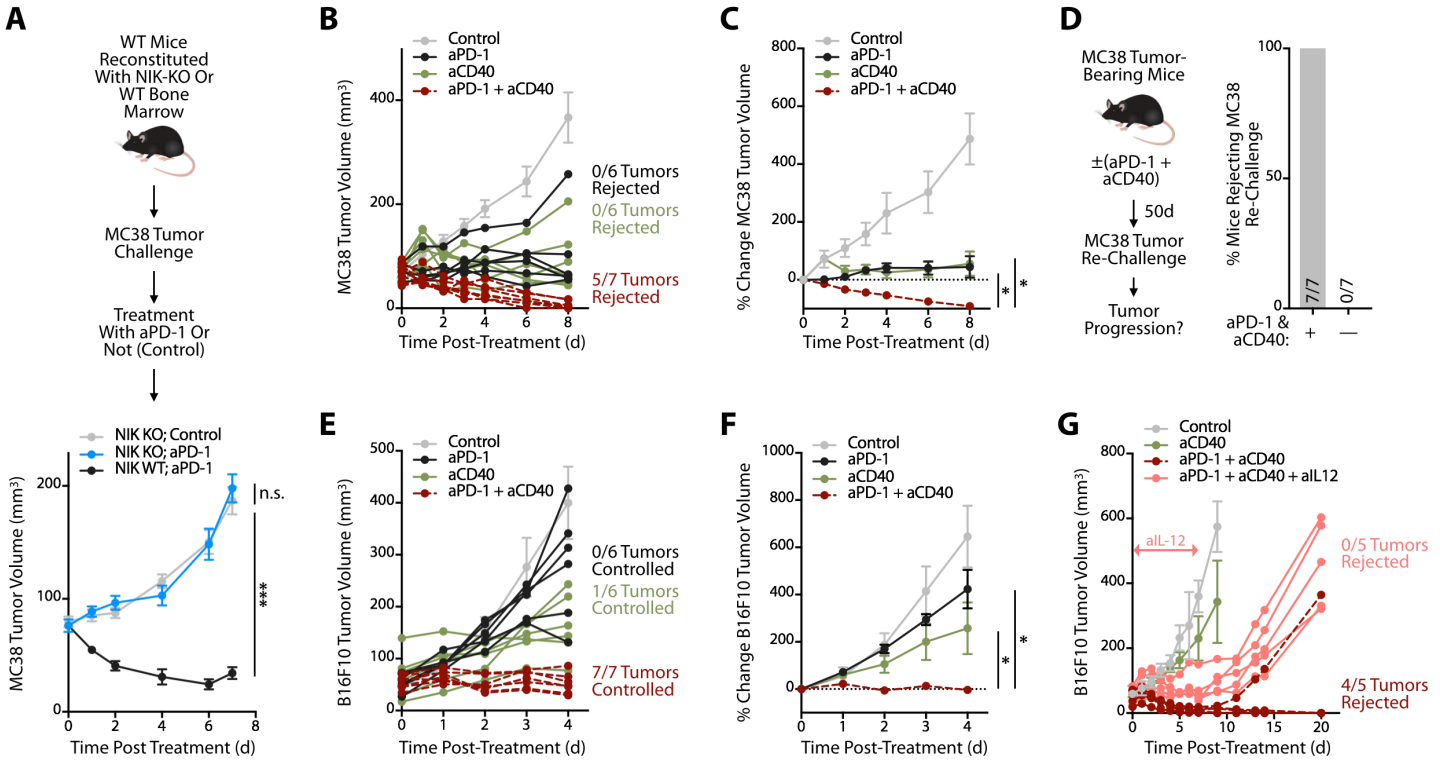

Fig. S7. Related to Figure 7. MC38 and B16 F10 Tumor Response to aPD-1 + aCD40 Combination Therapy. (A) Bone marrow chimeras reconstituted with either NIK KO or WT bone marrow were implanted with MC38 tumors and treated with aPD-1. NIK KO reconstituted mice not treated with aPD-1 were used as additional controls. The plot shown below indicates tumor progression over time in the different experimental groups (n = 5-10 mice/group). **(B, C)** MC38 tumor growth in mice that received aPD-1 mAb (black line), agonistic aCD40 mAb (green line) or aPD-1 + aCD40 combination (red line). Untreated mice were used as controls (grey line). Tumors were approximately 75 mm^3 in size at initiation of treatment (n ≥ 6 mice/group). (B) shows tumor volumes; dots for black, green and red groups represent single mice. (C) shows percent change tumor volume when compared to pre-treatment data. **(D)** MC38 bearing animals that showed a complete response to aPD-1 + aCD40 combination treatment were re-challenged with MC38 tumor cell implantation 50 days following initial tumor rejection. Naive mice that had not been exposed to MC38 were used as controls (n = 7 mice/group). Data show the percentage of mice rejecting MC38 re-challenge. **(E and F)** B16F10 tumor growth in mice that received aPD-1 mAb (black line), agonistic aCD40 mAb (green line) or aPD-1 + aCD40 combination (red line). Untreated mice were used as controls (grey line). Tumors were approximately 75 mm^3 in size at initiation of treatment (n ≥ 6 mice/group). (E) shows tumor volumes; dots for black, green and red groups represent single mice. (F) shows percent change tumor volume when compared to pre-treatment data. **(G)** B16F10 tumor volume measurements in mice that received aCD40 (green line), aPD-1 + aCD40 (red dashed line) or aPD-1 + aCD40 + aIL-12 (pink line). Untreated mice served as controls (grey circles). Dots for red and pink groups represent single mice. n ≥ 5 mice/group. Results are representative of at least 2 independent experiments. * $p < 0.05$, ** $p < 0.01$, *** $p < 0.001$, One way ANOVA with multiple comparisons.